ChemPhysChem

Chemistry Europe
European Chemical Societies Publishing
ChemPhysChem

RESEARCH ARTICLE OPEN ACCESS

Valence Threshold Photoionization Spectra of C_5H and C_5H_2 Isomers

Ugo Jacovella[1] | Myriam Drissi[2] | Bérenger Gans[1] | Corentin Rossi[1] | Gustavo A. Garcia[2] | Hai Linh Le[1] | Mengxu Jiang[1] | Jean-Claude Guillemin[3] | Séverine Boyé-Péronne[1] | Jean-Christophe Loison[4]

[1]Université Paris-Saclay, CNRS, Institut des Sciences Moléculaires d'Orsay, Orsay, France | [2]Synchrotron SOLEIL, L'Orme des Merisiers, Saint-Aubin, France | [3]Univ Rennes, Ecole Nationale Supérieure de Chimie de Rennes, CNRS, ISCR UMR6226, Rennes, France | [4]Université Bordeaux, CNRS, Bordeaux INP, ISM, Talence, France

Correspondence: Ugo Jacovella (ugo.jacovella@universite-paris-saclay.fr) | Jean-Christophe Loison (jean-christophe.loison@cnrs.fr)

Received: 10 February 2026 | **Revised:** 13 March 2026 | **Accepted:** 15 March 2026

Keywords: C_5H | C_5H_2 | photoionization | TPEPICO

ABSTRACT

C_5H_x species are important intermediates in the formation of large carbonaceous molecules. Mass-selected threshold photoelectron spectra (TPES) of l-C_5H, HC_5H, and c–C_3H–CCH were recorded using double-imaging photoelectron–photoion coincidence spectroscopy. The TPES of l-C_5H and c–C_3H–CCH are reported for the first time. These transient species were generated in situ by hydrogen abstraction from cyclopropylacetylene and 1,3-pentadiyne by fluorine atoms in a discharge flow-tube reactor. Supported by *ab initio* calculations and Franck–Condon simulations, unambiguous assignments were achieved, enabling accurate determination of adiabatic ionization energies. The C_5H_2 results show that hydrogen abstraction from structurally distinct precursors leads to similar isomeric distributions. More generally, the high-resolution TPES fingerprints reported here provide reliable discrimination between linear and cyclic C_5H_x isomers, which is not possible using only photoion yields, offering robust benchmarks for identifying reactive hydrocarbon intermediates in combustion and astrochemical environments.

1 | Introduction

Due to their potentially high reactivity, the C_5H radical [1] and, to a lesser extent, C_5H_2 are promising sources for hydrocarbon growth in combustion environments [2] and in the interstellar medium, where certain C_5H and C_5H_2 isomers have been detected [3–7]. Hydrocarbon radicals with an odd number of carbon atoms typically exhibit different chemical properties than those with an even number. The key role and chemical richness of C_3H and C_3H_2 species in interstellar environments have been well established [8]. As is often the case for small hydrocarbons, these species are relevant in both combustion processes [2] and astrochemistry, where C_5H_2 can be produced through the C + C_4H_2 reaction [9] and the C_3 + C_2H_3 reaction [10].

C_5H exists primarily in two distinct structural forms: a linear configuration (l-C_5H) and a cyclic isomer (c-C_5H). The cyclic form consists of a three-membered ring with an attached C_2H unit. According to coupled-cluster calculations, the linear structure is slightly more stable (by 0.26 eV using DZP basis set [11] or 0.35 eV using aug-cc-pVTZ basis set [12]). l-C_5H was first discovered in the expanding envelope of the carbon-rich star IRC + 10 216 [3] and soon after in the dense molecular cloud TMC-1 [4]. However, c-C_5H was only detected in TMC-1 in 2022 [5].

Early chemical models [13] did not account for the cyclic isomer. In these models, l-C_5H was thought to form either through dissociative electron attachment to $C_5H_3^+$—whose detection is still pending—or *via* C_2H addition/H elimination reactions involving C_4H. Following the detection of c-C_5H, its formation was incorporated into the latest UMIST network [14] through the reaction of atomic carbon with C_4H_2, yielding ≈ 10% of the cyclic isomer.

The history of discoveries of C_5H_2 species is particularly surprising, as numerous stable isomers have been theoretically predicted

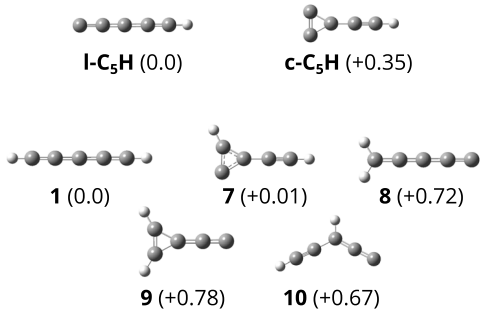

FIGURE 1 | The two most stable C_5H isomers with their relative energies (in eV, Ref. [12]) as well as five C_5H_2 isomers with the relative energies (in eV) and the notation as in Ref. [19]. For C_5H_2 isomers, isomer (**1**) has a triplet ground state, and all others are singlets.

[2, 15–18], yet only five have been experimentally confirmed (see Figure 1) [1, 19–26] (we have retained the notation of Ref. [19]). Notably, the first detected isomer in interstellar media was the third most stable labeled isomer (**8**) in Figure 1 (H_2C_5) [6], in contrast to the case of C_5H, where the most stable isomer was identified first. The most stable cyclic isomer (**7**) was, however, detected just after [7] with a notably larger abundance in TMC-1.

These synthesized species cannot be stored in our experiment and thus were generated in situ and studied in operando. There are two known possible ways to produce these species, either through chemical reactivity (this work) or unimolecular decomposition [19]. In both cases, the chemistry is controlled by kinetics, with the most favorable reaction pathways being those with the lowest energy paths (i.e., the lower transition state hills to climb) rather than those that are the most exothermic (in some cases, they are the same, but not necessarily). This is why the most stable isomers are not always the ones produced.

Tunable vacuum ultraviolet (VUV) mass spectrometry allows probing the reaction products by monitoring the photoion yield as a function of photon energy in a mass-selective manner [27]. It has been successfully applied to investigate fuel-rich flame chemistry involving C_5H_2 species [2], as well as the growth of odd hydrogenated carbon chains through acetylene addition in the context of dense molecular cloud chemistry [1].

This approach is particularly effective when the number of isomeric products is limited, their ionization energies are well separated, and they exhibit sharp photoionization thresholds that allow for straightforward identification. However, challenges arise when these conditions are not met. These difficulties can be overcome by probing reaction products using their threshold photoelectron spectrum (TPES) [28], which provides a much more sensitive fingerprint [29]. Nevertheless, this method requires prior knowledge of the spectral fingerprints, which can be difficult to obtain for such elusive species, although a database has been recently created for this specific need [30].

To date, no TPES of C_5H has been reported. Only a photoionization yield spectrum has been measured [1], showing a slow and gradual rise. This allowed for the identification of l-C_5H based on density functional theory (DFT) calculations, but prevented an unambiguous assessment of the presence of c-C_5H. Recently, more advanced calculations have been performed, yielding ionization energies of 8.36 and 9.11 eV for the linear and cyclic isomers, respectively [12].

For C_5H_2, slightly more experimental data are available. A similar photoionization yield spectrum has been recorded [1], but assigning the structures responsible for it remains highly challenging. This complexity arises from the large number of possible C_5H_2 isomers that can form in both singlet and triplet states, significantly increasing the number of potential species present. However, a TPES of C_5H_2 obtained from flash pyrolysis of a diazo precursor has been reported and provides the unambiguous fingerprint of the HC_5H isomer (**1**) and a tentative assignment of a high-lying energy cyclic isomer (**9**) [19].

In this paper, we present the TPES of C_5H and C_5H_2 species generated by hydrogen abstraction from two precursors using fluorine atoms. This work provides the first TPES of C_5H and identifies the fingerprint of a third C_5H_2 isomer (**7**) while confirming the previous assignment for the isomer (**1**) of C_5H_2.

2 | Methodologies

2.1 | Experimental Setup

The experiments were performed at the SOLEIL French synchrotron facility, on the DESIRS beamline [31], and have been described in detail in previous works [32, 33]. The method relies on the high reactivity of fluorine atoms in the gas phase with hydrocarbons containing C–H single bonds [34]. This reactivity allows hydrogen atoms to be abstracted, forming HF and a radical. By using fluorine atom concentrations close to those of the hydrocarbons, we can abstract multiple hydrogen atoms and generate highly unsaturated carbon-based radicals, such as C_3, C_3H and C_3H_2 from CH_3CCH [35], as well as C_2N and HCCN from CH_3CN [36]. We employed this method to abstract multiple hydrogen atoms from c-C_5H_6 and 1-3-pentadiyne to produce the C_5H and C_5H_2 radicals. Cyclopropylacetylene (c-C_5H_6) precursor was purchased from Sigma–Aldrich and was used without further purification (97% purity). 1,3-pentadiyne (CH_3C_4H) precursor was prepared according to the method developed by Kerisit et al. [37] and transported to the SOLEIL synchrotron facility in a cell under dry nitrogen, closed by a stopcock, and immersed in dry ice. Cyclopropylacetylene, or 1,3-pentadiyne, was swept into a quartz reactor with a continuous flow of helium (1000 sccm, standard cubic centimeters per minute), while fluorine atoms were produced by microwave discharge of a 5% F_2/He mixture and fed into a quartz shower-head injector that slides into the center of the reactor. The use of F_2 is subject to approval by the safety officers at the SOLEIL synchrotron and is conditional on the permanent presence of an F_2 leak detector. The final pressure in the reactor was 1 mbar. The concentrations of cyclopropylacetylene and 1,3-pentadiyne were estimated at 1×10^{14} molecules·cm^{-3}. The concentration of F atoms was estimated at 2×10^{13} molecules·cm^{-3}. The contents of the reactor were then expanded through a 1-mm skimmer into an intermediate vacuum chamber (10^{-4} mbar). The distance between injector and skimmer gave the reaction time, which was of the order of a few milliseconds. The molecular beam then traversed a second skimmer before reaching the center of the DELICIOUS3 i^{2}PEPICO spectrometer [38], where it intersected the synchrotron beam. Ions and electrons were extracted in opposite directions by a DC field of 88.7 V/cm, detected by velocity map imaging detectors, and correlated in time so that the photoelectron images could be mass-tagged. At each photon energy, the

mass-selected photoelectron spectra were extracted from the images with an Abel inversion algorithm [38]. In an energy scan, the coincident signal as a function of electron kinetic energy and photon energy was recorded and could be reduced to an TPES using a previously reported methodology [36]. The photon and electron bandwidths chosen in this work led to a total energy resolution of 20 meV for C_5H and 12 meV for C_5H_2 for the TPES presented here. A gas filter filled with Kr cut off the high harmonic radiations from the undulator, ensuring spectral purity. The energy scans were corrected by the photon flux as measured by a dedicated photodiode (AXUV, IRD) as well as by fast total yield scans to correct smooth variations in the flow tube reactor. The energy scale was calibrated using the Ionization Energy (IE) of CH_3 [39] for C_5H spectra and with the IE of CF [40] for C_5H_2 spectra, these radicals (CH_3 and CF) being produced in the reactor at the same time.

2.2 | Calculations

The Franck-Condon (FC) factors for photoionization were calculated using the standard FC factors procedure of Gaussian 2016 software [41] with geometry optimization and harmonic frequency calculations performed at the DFT level applying the M06-2X functional and the aug-cc-pVTZ basis set. The chemical method used to produce C_5H and C_5H_2 is not inherently selective, and we can produce several isomers. To assign the spectra, we first deduce the molecular formulas corresponding to the observed masses ($m/z = 61$ and 62), considering our starting points for the abstraction reactions (C_5H_6 + F and C_5H_4 + F). This eliminates fluorinated compounds corresponding to these masses (e.g., C_3H_6F, C_3H_7F, and C_2F_2), which would require overly complex formation mechanisms. Furthermore, the observed cations are clearly not from fragmentation, as shown by the mass peak shape, which is logical as we work at low photon energies, which rules out the possibility of fragmentation from larger ions. Therefore, we assign the masses $m/z = 61$ and 62 to C_5H and C_5H_2, respectively. The observed spectra are assigned to specific isomers by comparing the experimental results with theoretically simulated photoelectron spectra. This process involves not only matching the calculated and experimental ionization energies but also examining and comparing the overall spectral shapes and features, primarily due to vibrational progressions, given the total energy resolution of 20 meV for C_5H and 12 meV for C_5H_2. For C_5H, considering the precision of DFT calculations, we performed RCCSD(T) calculations of the adiabatic ionization energies using the aug-cc-pVTZ basis set and MOLPRO 2015 package [42] to secure the assignments. The T1 diagnostic value ranges between 0.016 and 0.035, indicating that the RCCSD(T) calculations are relatively accurate [43]. For the C_5H_2 isomers, we used our DFT calculations along with previous ones [2, 19].

3 | Results and Discussion

3.1 | C_5H

Figure 2 (top panel) presents the experimental TPES corresponding to the ions with m/z 61 using 1,3-pentadiyne (CH_3C_4H) as a precursor. The TPES of both l-C_5H and c-C_5H have been computed for excitation from the ground electronic state of the neutral toward the lowest singlet and triplet electronic states of the corresponding cations, and they are displayed in the lower panels of Figure 2. The only unambiguous identification is the presence of l-C_5H, identified through the $X^+\ ^1\Sigma^+ \leftarrow X\ ^2\Pi$ photoionizing transition. The spectrum is dominated by a strong origin band with almost no vibrational progressions due to similar geometries for the neutral and ionic l-C_5H, which is well reproduced by our theoretical spectrum. The adiabatic ionization energy is then determined to be 8.516 ± 0.005 eV, relatively close to our calculated value of 8.68 eV at M06-2X/aug-cc-pVTZ level and 8.40 eV at RCCSD(T)/aug-cc-pVTZ level, reported in Table 1. The good agreement between the theoretical and experimental IE values, combined with the strong match in the theoretical and experimental spectral profile dominated by a single vibrational transition, secures the assignment of the observed spectrum near 8.5 eV to l-C_5H. Due to the signal-to-noise ratio, c-C_5H assignment is not possible. However, the next prominent peak around 10.1 eV could potentially correspond to the origin band of the photoionization transition toward the $a^+\ ^3\Pi$ state, the value being close to the calculated one. Nevertheless, the absence of measurements in the higher-energy region where a strong vibronic transition was expected prevents the assignment of the $a^+\ ^3\Pi \leftarrow X\ ^2\Pi$ transition.

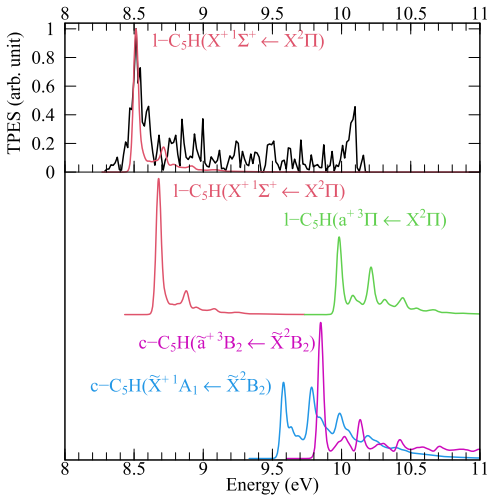

FIGURE 2 | Mass-selected experimental TPES of C_5H compared to Franck-Condon simulations for the linear and cyclic isomers. The relative intensities of the simulations have been adjusted to reproduce the experimental trace. In the upper plot, the simulated spectrum of the $X^+\ ^1\Sigma^+ \leftarrow X\ ^2\Pi$ transition of l-C_5H has been shifted by -0.164 eV in order to reproduce the band position. In the lower panels, the various transitions are plotted with a position given by our M06-2X/aug-cc-pVTZ calculations (see Table 1) and an intensity normalized over the integral of the spectra for each transition for a given isomer, considering identical photoionization cross-sections.

3.2 | C_5H_2

Figure 3 presents the TPES corresponding to the ion with m/z 62 using 1,3-pentadiyne (CH_3C_4H) as precursor. The simulated photoelectron spectra of the five experimentally observed isomers, shown in Figure 1, are also displayed in the lower panels. The linear isomer (**1**) can be unambiguously identified, as its spectrum is dominated by the origin transition at 8.381

TABLE 1 | Adiabatic IE in eV calculated in this work for the two most stable C_5H isomers, compared with the experimental value determined from the TPES.

Isomer	Photoionizing transition	IE(M06-2X)[a]	IE(CCSD(T))[b]	T1[c]	IE_{exp}
l–C_5H	$X^+\,^1\Sigma^+ \leftarrow X\,^2\Pi$	8.68	8.40	0.035	8.516 ± 0.005
	$a^+\,^3\Pi \leftarrow X\,^2\Pi$	9.98	10.08	0.022	—
c–C_5H	$\tilde{X}^+\,^1A_1 \leftarrow \tilde{X}\,^2B_2$	9.58	9.20	0.016	—
	$\tilde{a}^+\,^3B_2 \leftarrow \tilde{X}\,^2B_2$	9.85	9.78	0.027	—

[a]M06-2X/aug-cc-pVTZ including Zero Point Energy (ZPE);
[b]RCCSD(T)/aug-cc-pVTZ with ZPE calculated at M06-2X/aug-cc-pVTZ;
[c]T1 diagnostic, definition in [43].

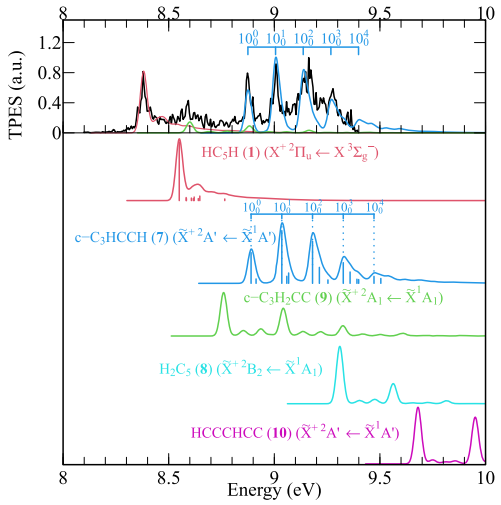

FIGURE 3 | Mass-selected experimental TPES compared with Franck-Condon simulations of the first photoionizing transition of the C_5H_2 isomers depicted in Figure 1. In the upper plot, the position and the relative intensities of the simulations for isomers (**1**) and (**7**) have been adjusted to reproduce the experimental trace (see Table 2 for the various theoretical predictions). The position of the transition for the isomer (**9**) is from Reusch et al. [19]. The vibrational progression of the c-C_3H-C_2H (**7**) was multiplied by 0.91. In the lower plot, the various transitions are plotted with a position given by our M06-2X/aug-cc-pVTZ calculations (see Table 2) and with arbitrary intensities.

$\pm$ 0.005 eV, consistent with the observations of Reusch et al. [19] (8.36 $\pm$ 0.03 eV) and our FC calculations (see Table 2). The band system spanning from 8.9 to 9.4 eV is unambiguously assigned to the cyclic isomer (**7**), based on our quantum chemical calculations and FC calculations at the M06-2X/aug-cc-pVTZ level. Indeed, the spectral profile cannot be attributed to any other species, highlighting the importance of accurately reproducing theoretically the vibronic transitions observed in the photoelectron spectra to fully take advantage of these unique fingerprints. The four peaks spaced by 1060 cm^{-1} clearly correspond to the vibrational progression associated with the bending mode of the three-carbon ring in isomer (**7**) (ν_{10} vibrational mode from Gaussian output file), as demonstrated by our FC simulation in Figure 3. The theoretical M06-2X/aug-cc-pVTZ value of this mode is equal to 1163 cm^{-1}, which is in good agreement once the scaling factor [44] is applied to the calculated vibrational frequencies (0.91 in our case). Additional structures are also discernible, which could likely be attributed to combination bands involving other ring deformations (vibrational modes ν_{11} and ν_{12}), but the signal-to-noise ratio in our spectrum prevents their precise identification. The IE is determined to be equal to 8.875 $\pm$ 0.005 eV. The experimental spectrum presented in Figure 3 was recorded using 1,3-pentadiyne (CH_3C_4H) as a precursor. However, note that cyclopropylacetylene (c – C_5H_6) was also employed, and the resulting C_5H_2 TPES recorded with this precursor was very similar. It therefore appears that the ratio between isomer (**1**) linear HC_5H and isomer (**7**) cyclic

TABLE 2 | Calculated and experimental adiabatic IE in eV for various C_5H_2 isomers (the integers in parentheses for the isomers of C_5H_2 are the labels used in Figure 1).

Isomer	Ion transition	IE(M06)[a]	IE(QCISD(T))[b]	IE(CCSD(T))[c]	IE(CASPT2)[d]	IE_{exp}
HC_5H (**1**)	$X^+\,^2\Pi_u \leftarrow X\,^3\Sigma_g^-$	8.55	8.39	8.26	8.20	8.381 ± 0.005[e]
						8.36 ± 0.03[f]
c–C_3HCCH (**7**)	$\tilde{X}^+\,^2A' \leftarrow \tilde{X}\,^1A'$	8.89	—	8.77	8.70	8.875 ± 0.005[e]
c–C_3H_2CC (**9**)	$\tilde{X}^+\,^2A_1 \leftarrow \tilde{X}\,^1A_1$	8.76	—	9.96	8.55	8.60 ± 0.03[f]
H_2C_5 (**8**)	$\tilde{X}^+\,^2B_2 \leftarrow \tilde{X}\,^1A_1$	9.31	9.48	9.40	9.10	—
HCCCHCC (**10**)	$\tilde{X}^+\,^2A' \leftarrow \tilde{X}\,^1A'$	9.68	—	8.92	9.62	—

[a]M06-2X/aug-cc-pVTZ, this work;
[b]QCISD(T)/aug-cc-pVQZ with ZPE calculated at B3LYP/6-311++G(d,p) [2];
[c]CCSD(T)/aug-cc-pVTZ with ZPE calculated at ωB97xD/6-311++G(d,p) [19];
[d]CASPT2/cc-pVTZ//ωB97xD/6-311G) [19];
[e]this work;
[f]from Ref. [19].

c-$C_3H - C_2H$ depends little on the precursor, whether it is cyclic or not. Isomers (**1**) and (**7**) have very similar calculated energies [2, 18] and are the most stable C_5H_2 isomers, but the linear isomer (**1**) is likely kinetically favored since cyclization is generally entropically disfavored. However, isomer (**1**) has a triplet ground state with a singlet state significantly higher in energy. Thus, while isomer (**1**) is probably favored when the reaction F + C_5H_4 occurs on the triplet surface, the cyclic isomer (**7**)—which is the most stable singlet isomer—should be favored when the abstraction reaction takes place on the singlet surface. The spectral fingerprints of isomers (**8**) and (**10**) were not measured, as they fall within the energy range where the photoionizing transitions of the precursor begin. Therefore, no information can be provided regarding the potential formation of these isomers from this precursor. Isomer (**9**) has previously been assigned to the band around 8.6 eV [19]. Based on our experimental spectrum, however, we cannot make a definitive statement regarding the presence or absence of this isomer. The band observed around 8.6 eV could originate from isomer (**9**), from vibronic transitions not captured by the harmonic FC calculations of isomer (**1**), or from a combination of both contributions.

4 | Conclusion

We have recorded mass-selected threshold photoelectron spectra of the l-C_5H, HC_5H, and c–C_3H–CCH, species using double-imaging photoelectron–photoion coincidence detection technique. The TPES of l-C_5H and c–C_3H–CCH are reported for the first time. These transient species were generated in situ by hydrogen abstraction from cyclopropylacetylene and 1,3-pentadiyne by fluorine atoms in a discharge flow-tube reactor.

Supported by *ab initio* calculations and Franck–Condon simulations, unambiguous assignments were achieved, yielding accurate adiabatic ionization energies. The ionization energies of l-C_5H and c–C_3H–CCH were determined for the first time to be 8.516 ± 0.005 eV and 8.875 ± 0.005 eV, respectively, while that of HC_5H was measured as 8.381 ± 0.005 eV, in good agreement with the value of Reusch et al., equal to 8.36 ± 0.03 eV [19].

The C_5H_2 results demonstrate that hydrogen abstraction from different precursors leads to remarkably similar isomeric distributions, suggesting that the branching between linear HC_5H and cyclic c–C_3H–CCH is only weakly sensitive to the molecular structure of the precursor. This observation highlights the interplay between thermodynamic stability, spin multiplicity, and reaction dynamics in governing isomer formation. In particular, the coexistence of isomers with a triplet linear ground state and isomers with a singlet cyclic ground state suggests that abstraction reactions proceeding on different spin surfaces may contribute to the observed product mixture.

More generally, this study highlights the crucial role that threshold photoelectron spectroscopy can play as a diagnostic tool for identifying reactive intermediates. Although accurate ionization energies are essential for species identification in complex environments such as flames or chemical reactors, they are often insufficient for accurate isomer discrimination. The availability of high-resolution TPES fingerprints, as demonstrated here, could substantially enhance the identification of elusive hydrocarbon radicals and carbenes in laboratory experiments, as illustrated by the reliable discrimination between linear and cyclic C_5H_x isomers. These data provide robust benchmarks for the identification of C_5H_x radicals in laboratory studies and offer valuable constraints for models of carbon-chain growth in combustion and astrochemical environments.

Acknowledgments

This work was performed on the DESIRS beamline at SOLEIL synchrotron under proposal number #20231200. We are grateful to the whole staff of SOLEIL for running the facility. M. D. and M. J. acknowledge the financial support of the French "Agence Nationale de la Recherche" (ANR) under grant no. ANR-21-CE29−0017 (Project ZEPHIRS) for their post-doctoral fellowship grants. J.-C.G. thanks the Programme National "Physique et Chimie du Milieu Interstellaire" (PCMI) of CNRS/INSU with INC/INP cofunded by Commissariat à l'énergie atomique et aux énergies alternatives (CEA) and Centre national d'études spatiales (CNES) for a grant.

Open access publication funding provided by COUPERIN CY26.

Funding

This study was supported by Agence Nationale de la Recherche (ANR-21-CE29-0017) and PCMI.

Conflicts of Interest

The authors declare no conflicts of interest.

Data Availability Statement

The data that support the findings of this study are available from the corresponding author upon reasonable request.

References

1. Y.-L. Sun, W.-J. Huang, and S.-H. Lee, "Formation of C_3H_2, C_5H_2, C_7H_2, and C_9H_2 from Reactions of CH, C_3H, C_5H, and C_7H Radicals with C_2 H_2," *Physical Chemistry Chemical Physics* 18 (2016): 2120.

2. N. Hansen, S. J. Klippenstein, J. A. Miller, et al., "Identification of C_5H_x Isomers in Fuel-Rich Flames by Photoionization Mass Spectrometry and Electronic Structure Calculations," *The Journal of Physical Chemistry. A* 110 (2006): 4376.

3. J. Cernicharo, C. Kahane, J. Gomez-Gonzalez, and M. Guélin, "Detection of the $2Pi_{3/2}$ State of C_5H," *Astronomy and Astrophysics* 164 (1986): L1.

4. J. Cernicharo, M. Guélin, and C. Walmsley, "Detection of the Hyperfine Structure of the C_5H Radical," *Astronomy and Astrophysics* 172 (1987): L5.

5. C. Cabezas, M. Agúndez, R. Fuentetaja, et al., "Discovery of the Cyclic C_5H Radical in TMC-1," *Astronomy and Astrophysics* 663 (2022): L2.

6. C. Cabezas, B. Tercero, M. Agúndez, et al., "Cumulene Carbenes in TMC-1: Astronomical Discovery of *l* -H_2C_5," *Astronomy and Astrophysics* 650 (2021): L9.

7. J. Cernicharo, M. Agúndez, C. Cabezas, et al., "Pure Hydrocarbon Cycles in TMC-1: Discovery of Ethynyl Cyclopropenylidene, Cyclopentadiene, and Indene," *Astronomy & Astrophysics* 649 (2021): L15.

8. J.-C. Loison, M. Agúndez, V. Wakelam, et al., "The Interstellar Chemistry of C_3H and C_3H_2 Isomers," *Monthly Notices of the Royal Astronomical Society* 470 (2017): 4075.

9. B. J. Sun, C. Y. Huang, H. H. Kuo, et al., "Formation of Interstellar 2,4-Pentadiynylidyne, HCCCCC(XΠ2), via the Neutral-Neutral Reaction of Ground State Carbon Atom, C(P3), with Diacetylene, HCCCCH(XΣg+1)," *The Journal of Chemical Physics* 128 (2008): 244303.

10. I. A. Medvedkov, A. A. Nikolayev, S. J. Goettl, Z. Yang, A. M. Mebel, and R. I. Kaiser, "From the laboratory to Space: Unveiling Isomeric Diversity of C_5H_2 in the Reaction of Tricarbon (C_3, $X^1\Sigma_g^+$) with the Vinyl Radical (C_2H_3, X^2A')„," *Chemical Science* 16 (2025): 17859–17866, https://pubs.rsc.org/en/content/articlelanding/2025/sc/d5sc04699h.

11. T. D. Crawford, J. F. Stanton, J. C. Saeh, and H. F. Schaefer, "Structure and Energetics of Isomers of the Interstellar Molecule C_5h," *Journal of the American Chemical Society* 121 (1999): 1902.

12. S. Satpati, T. Roy, A. Anoop, V. S. Thimmakondu, and S. Ghosal, "Energetic and Spectroscopic Properties of the Low-Lying Isomers of C_5H: A High-Level Ab Initio Study," *Atoms* 11 (2023): 115.

13. B. Turner, E. Herbst, and R. Terzieva, "The Physics and Chemistry of Small Translucent Molecular Clouds. XIII. The Basic Hydrocarbon Chemistry," *The Astrophysical Journal Supplement Series* 126 (2000): 427.

14. T. Millar, C. Walsh, M. Van de Sande, and A. Markwick, "The UMIST Database for Astrochemistry 2022," *Astronomy and Astrophysics* 682 (2024): A109.

15. R. A. Seburg, R. J. McMahon, J. F. Stanton, and J. Gauss, "Structures and Stabilities of C_5H_2 Isomers: Quantum Chemical Studies," *Journal of the American Chemical Society* 119 (1997): 10838.

16. V. S. Thimmakondu, I. Ulusoy, A. K. Wilson, and A. Karton, "Theoretical Studies of Two Key Low-Lying Carbenes of C_5H_2 Missing in the Laboratory," *The Journal of Physical Chemistry. A* 123 (2019): 6618.

17. A. G. Watrous, B. R. Westbrook, and R. C. Fortenberry, "Theoretical Spectra and Energetics for c-C_3HC_2H, l-C_5H_2, and Bipyramidal D3h C_5H_2," *Frontiers in Astronomy and Space Sciences* 9 (2022): 1051535.

18. V. S. Thimmakondu and A. Karton, "CCSD(T) Rotational Constants for Highly Challenging C_5H_2 Isomers—A Comparison between Theory and Experiment," *Molecules* 28 (2023): 6537.

19. E. Reusch, D. Kaiser, D. Schleier, et al., "Pentadiynylidene and Its Methyl-Substituted Derivates: Threshold Photoelectron Spectroscopy of R_1-C_5-R_2 Triplet Carbon Chains," *The Journal of Physical Chemistry. A* 123 (2019): 2008.

20. J. Fulara, P. Freivogel, D. Forney, and J. P. Maier, "Electronic Absorption Spectra of Linear Carbon Chains in Neon Matrices. III. $HC_{2n+1}H$," *The Journal of Chemical Physics* 103 (1995): 8805.

21. M. McCarthy, M. Travers, A. Kovács, et al., "Detection and Characterization of the Cumulene Carbenes H_2C_5 and H_2C_6," *Science (New York, N.Y.)* 275 (1997): 518.

22. M. J. Travers, M. McCarthy, C. Gottlieb, and P. Thaddeus, "Laboratory Detection of the Ring-Chain Molecule C_5H," *The Astrophysical Journal* 483 (1997): L135.

23. S. J. Blanksby, S. Dua, J. H. Bowie, D. Schröder, and H. Schwarz, "Gas-Phase Syntheses of Three Isomeric C_5H_2 Radical Anions and Their Elusive Neutrals. A Joint Experimental and Theoretical Study," *The Journal of Physical Chemistry. A* 102 (1998): 9949.

24. C. Gottlieb, M. McCarthy, V. D. Gordon, J. Chakan, A. Apponi, and P. Thaddeus, "Laboratory Detection of Two New C_5H_2 Isomers," *The Astrophysical Journal* 509 (1998): L141.

25. N. P. Bowling, R. J. Halter, J. A. Hodges, et al., "Reactive Carbon-Chain Molecules: Synthesis of 1-Diazo-2,4-Pentadiyne and Spectroscopic Characterization of Triplet Pentadiynylidene (H−CC−C−CC−H)," *Journal of the American Chemical Society* 128 (2006): 3291.

26. M. Steglich, J. Fulara, S. Maity, A. Nagy, and J. P. Maier, "Electronic Spectra of Linear HC_5H and Cumulene Carbene H_2C_5," *The Journal of Chemical Physics* 142 (2015): 244311.

27. D. L. Osborn, P. Zou, H. Johnsen, et al., "The Multiplexed Chemical Kinetic Photoionization Mass Spectrometer: A New Approach to Isomer-Resolved Chemical Kinetics," *The Review of Scientific Instruments* 79 (2008): 104103.

28. A. Bodi, P. Hemberger, D. L. Osborn, and B. Sztáray, "Mass-Resolved Isomer-Selective Chemical Analysis with Imaging Photoelectron Photoion Coincidence Spectroscopy," *The Journal of Physical Chemistry Letters* 4 (2013): 2948.

29. H. R. Hrodmarsson, G. A. Garcia, L. Bourehil, et al., "The Isomer Distribution of C_6H_6 Products from the Propargyl Radical Gas-Phase Recombination Investigated by Threshold-Photoelectron Spectroscopy," *Communications Chemistry* 7 (2024): 156.

30. P. Hemberger, Z. Pan, X. Wu, Z. Zhang, K. Kanayama, and A. Bodi, "Photoion Mass-Selected Threshold Photoelectron Spectroscopy to Detect Reactive Intermediates in Catalysis: From Instrumentation and Examples to Peculiarities and a Database," *The Journal of Physical Chemistry C* 127 (2023): 16751, https://doi.org/10.1021/acs.jpcc.3c03120.

31. L. Nahon, N. de Oliveira, G. A. Garcia, et al., "DESIRS: A State-of-the-Art VUV Beamline Featuring High Resolution and Variable Polarization for Spectroscopy and Dichroism at SOLEIL," *Journal of Synchrotron Radiation* 19 (2012): 508.

32. G. A. Garcia, B. Gans, X. Tang, et al., "Threshold Photoelectron Spectroscopy of the Imidogen Radical," *Journal of Electron Spectroscopy and Related Phenomena* 203 (2015): 25.

33. G. A. Garcia, X. Tang, J.-F. Gil, et al., "Synchrotron-Based Double Imaging Photoelectron/Photoion Coincidence Spectroscopy of Radicals Produced in a Flow Tube: OH and OD," *The Journal of Chemical Physics* 142 (2015): 164201.

34. R. Foon and G. P. Reid, "Kinetics of the Gas Phase Fluorination of Hydrogen and Alkanes," *Transactions of the Faraday Society* 67 (1971): 3513.

35. G. A. Garcia, B. Gans, J. Kruger, et al., "Valence Shell Threshold Photoelectron Spectroscopy of C_3H_x (x = 0–3)," *Physical Chemistry Chemical Physics* 20 (2018): 8707.

36. G. A. Garcia, J. Krüger, B. Gans, C. Falvo, L. H. Coudert, and J.-C. Loison, "Valence Shell Threshold Photoelectron Spectroscopy of the CHCN (x = 0-2) and CNC Radicals," *The Journal of Chemical Physics* 147 (2017): 013908.

37. N. Kerisit, L. Toupet, Y. Trolez, and J.-C. Guillemin, "Methylcyanobutadiyne: Synthesis, X-ray Structure and Photochemistry; Towards an Explanation of Its Formation in the Interstellar Medium," *Chemistry - A European Journal* 19 (2013): 17683.

38. G. A. Garcia, L. Nahon, and I. Powis, "Two-Dimensional Charged Particle Image Inversion Using a Polar Basis Function Expansion," *Review of Scientific Instruments* 75 (2004): 4989.

39. A. M. Schulenburg, C. Alcaraz, G. Grassi, and F. Merkt, "Rovibrational Photoionization Dynamics of Methyl and Its Isotopomers Studied by High-Resolution Photoionization and Photoelectron Spectroscopy," *The Journal of Chemical Physics* 125 (2006): 104310.

40. U. Jacovella, B. Ruscic, N. L. Chen, et al., "Refining the Thermochemical Properties of CF, SiF, and Their Cations by Combining Photoelectron Spectroscopy, Quantum Chemical Calculations, and the Active Thermochemical Tables Approach," *Physical Chemistry Chemical Physics* 25 (2023): 30838.

41. M. J. Frisch, G. W. Trucks, H. B. Schlegel, et al., *Gaussian 16 Revision C.01* (Wallingford, CT., 2016).

42. H.-J. Werner, P. J. Knowles, P. Celani, et al., *MOLPRO, version, a package of ab initio programs.*

43. T. J. Lee and P. R. Taylor, "A Diagnostic for Determining the Quality of Single-Reference Electron Correlation Methods," *International Journal of Quantum Chemistry* 36 (1989): 199.

44. K. K. Irikura, I. Johnson, D. Russell, R. N. Kacker, and R. Kessel, "Uncertainties in Scaling Factors for *Ab Initio* Vibrational Zero-Point Energies," *The Journal of Chemical Physics* 130 (2009): 114102.